Electronic Supplementary Information

Visible-Light-Driven Bistable Photoswitching with Enhanced Solid State NIR-Fluorescence for Multi-Level Optical Storage

Pan Hong, [a] Nuo-Hua Xie, [a,b] Kai Xiong, [a] Jing Liu, [a] Ming-Qiang Zhu, [a] and Chong Li *[a]

[a] Wuhan National Laboratory for Optoelectronics, School of Optical and Electronic Information, Huazhong University of Science and Technology, Wuhan 430074, China

[b] Jingdezhen Ceramic University, School of Materials Science and Engineering, 333403

* Corresponding Authors
E-mail: chongli@hust.edu.cn

1. EXPERIMENTAL

1.1 Materials

Unless otherwise noted, all reactions were carried out under nitrogen atmosphere in dried flasks. Commercially available starting materials, reagents and solvents were supplied or obtained from Aladdin Chemicals, Energy Chemical or Sinopharm Chemical Reagent Co., Ltd. Tetrahydrofuran (THF) and 1'4-dioxane were dried by using sodium wire-benzophenone distillation system. Purification of intermediates and final products was accomplished mainly using silica gel (200-300 mesh).

1.2 Synthesis

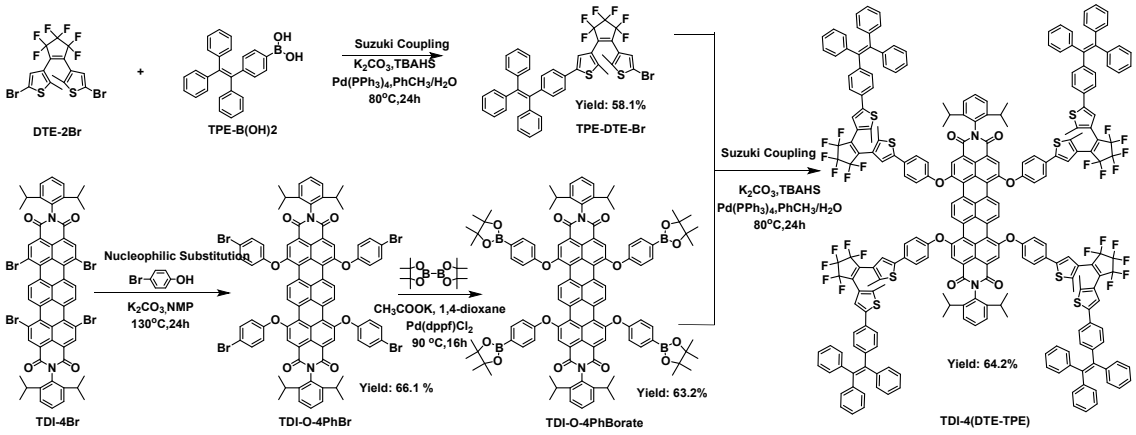

Scheme S1. Synthesis routes to TDI-4(DTE-TPE)

1,2-bis (5-bromo-2-methylthiophene-3-yl) perfluorocyclopentene (DTE-2Br) [1] and *N*,*N*'-di(2,6-diisopropylphenyl)-1,6,9,13-tetrabromo-terrylene-3,4,11,12-tetracarboxdiimides (TDI-4Br) [2] were prepared according to the previous works. The detailed synthesis procedures for other compounds (**Scheme S1**) are shown as follows：

Synthesis of TPE-DTE-Br

Under nitrogen atmosphere, DTE-2Br (2.52 g, 6.38 mmol), TPE-B$(OH)_2$ (1.50 g, 5.32 mmol) was dissolved in 80 mL toluene in a 250 mL double-moth flask. Then the water (40 mL) dissolved the potassium carbonate (2.76 g, 26.62 mmol) and a small amount of phase transfer catalyst (tetrabutylammonium hydrogen sulfate, TBAHS) was added. The reaction system was then vacuumed and filled with nitrogen which was repeated for three times. Subsequently, the catalyst Pd $(PPh_3)_4$ (0.24 g, 0.26 mmol)

was added under a stream of nitrogen carefully to ensure that the reaction system was oxygen-free. This mixture was heated at 80℃ for 24 h. After cooling down to room temperature, the obtained solution was extracted three times with dichloromethane and washed with water three times. The combined organic layer was dried over anhydrous sodium sulfate, then concentrated via an rotary evaporator, and further purified by silica gel column chromatography eluting with dichloromethane /petroleum ether (2 : 8 by volume) to yield a bit purple solid powder (1.80 g, 58.1 %). ^{1}H NMR (600 MHz, $CDCl_3$) δ 7.28 (s, 1H), 7.17 (s, 1H), 7.16-7.00 (m, 19H), 1.90 (d, *J* = 28.5 Hz, 6H). ^{13}C NMR (151 MHz, $CDCl_3$) δ 143.75, 143.69, 143.68, 143.61, 143.41, 142.44, 141.59, 141.21, 140.22, 132.11, 131.49, 131.45, 131.44, 131.17, 129.43, 128.00, 127.90, 127.79, 126.78, 126.73, 126.68, 125.64, 124.84, 122.03, 109.92, 14.73, 14.63. HR-MS: m/z calculated for $C_{41}H_{29}BrF_6S_2^+$ for $[M+H]^+$, 779.06, found 779.07 $[M+H]^+$

Synthesis of TDI-O-4PhBr

TDI-4Br (1.34 g, 1.17 mmol), *p*-bromophenol (1.21 g, 6.99 mmol), potassium carbonate (0.81 g, 5.82 mmol) and 125 mL *N*-methyl pyrrolidone (NMP) were added into 250 mL double-mouth flask under nitrogen atmosphere. The reaction system was then vacuumed and filled with nitrogen which was repeated for three times. The mixture was heating at 130 °C overnight. After cooling down to room temperature, the crude product was precipitated out spontaneously as low solubility at room temperature and filtered. This filter residue was washed with diluted hydrochloric acid, water, and ethanol, respectively. The obtained crude product was purified by silica gel column chromatography eluting with dichloromethane / petroleum ether (5 : 5 by volume) to yield a blue-black powder with metallic luster (1.17 g, 66.1 %). ^{1}H NMR (600 MHz, $CDCl^3$) δ 9.35 (s, 4H), 8.30 (s, 4H), 7.51-7.50 (m, 4H), 7.46 (t, *J* = 7.9 Hz, 2H), 7.34-7.30 (m, 8H), 7.03 (s, 4H), 6.72 (d, *J* = 8.9 Hz, 4H), 2.68 (dt, *J* = 13.6, 6.8 Hz, 4H), 1.14 (d, *J* = 6.8 Hz, 24H). ^{13}C NMR (151 MHz, $CDCl_3$) δ 162.77, 155.81, 154.78, 153.86, 145.55, 133.38, 132.46, 128.87, 128.74, 126.47, 124.34, 124.04, 124.02, 122.40, 120.62, 117.26, 117.17, 29.13, 24.03. MS (APCI, m/z): calculated for $C_{82}H_{58}Br_4N_2O_8^+$ for $[M]^+$ 1518.09, found 1518.09 $[M]^+$.

Synthesis of TDI-O-4PhBorate

TDI-O-4PhBr (1.0 g, 0.66 mmol), anhydrous potassium acetate (0.78 g, 7.95 mmol), bis(pinacol)diboron (1.17 g, 4.61 mmol) and anhydrous 1,4-dioxane (125 mL) were added into a 250 mL double-moth flask under nitrogen atmosphere. The reaction system was then vacuumed and filled with nitrogen which was repeated for three times. Then, the catalyst $Pd(dppf)Cl_2$ (0.10 g, 0.14 mmol) was added under a stream of nitrogen carefully to ensure that the reaction system was oxygen-free. This mixture was heated at 90 °C for 16 h. After cooling down to room temperature, the obtained solution was extracted with dichloromethane three times and washed with water three times. The combined organic layer was dried over anhydrous sodium sulfate, then concentrated via a rotary evaporator, and further purified by silica gel column chromatography eluting with dichloromethane /petroleum ether / ethyl acetate (5 : 5 : 1 by volume) to yield a cyan solid powder (0.71 g, 63.2 %). ^{1}H NMR (600 MHz, $CDCl_3$) δ 9.35 (s, 4H), 8.29 (s, 4H), 7.85 (d, *J* = 8.5 Hz, 8H), 7.44 (t, *J* = 7.8 Hz, 2H), 7.29 (d, *J* = 7.9 Hz, 4H), 7.14 (d, *J* = 8.5 Hz, 8H), 2.70 (dt, *J* = 13.7, 6.8 Hz, 4H), 1.34 (s, 48H), 1.13 (d, *J* = 6.8 Hz, 24H). ^{13}C NMR (151 MHz, $CDCl_3$) δ 162.84, 158.40, 153.81, 145.64, 137.16, 131.11, 130.55, 129.44, 128.84, 126.66, 124.67, 123.92, 122.20, 118.15, 83.89, 83.50, 29.07, 25.03, 24.86, 24.02. MS (APCI, m/z): calculated for $C_{106}H_{107}B_4N_2O_{16}^+$ for $[M+1]^+$ 1705.80, found 1706.80 $[M+1]^+$.

Synthesis of TDI-4(DTE-TPE)

TPE-DTE-Br (0.55 g, 0.70 mmol and TDI-O-4PhBorate (0.20 g, 0.12 mmol) was dissolved in 20 mL toluene in a 50 mL double-moth flask. Then the water (10 mL) dissolved the potassium carbonate (0.32 g, 2.32 mmol) and a small amount of TBAHS was added. The reaction system was then vacuumed and filled with nitrogen which was repeated for three times. Subsequently, the catalyst $Pd(PPh_3)_4$ (0.04 g, 0.04 mmol) was added under a stream of nitrogen carefully to ensure that the reaction system was oxygen-free. This reaction mixture was heated at 80℃ for 24 h. After cooling down to room temperature, the obtained solution was extracted three times with dichloromethane and washed with water three times. The combined organic layer was dried over anhydrous sodium sulfate, then concentrated via a rotary evaporator, and further purified by silica gel column chromatography eluting with dichloromethane / petroleum ether (6 : 4 by volume) to yield a bit purple solid powder (0.30 g, 64.2 %). ^{1}H NMR (600 MHz, CD_2Cl_2) δ 9.49 (s, 4H), 8.31 (s, 4H), 7.60 (d, J = 8.6 Hz, 8H),

7.47 (t, J = 7.9 Hz, 2H), 7.30 (dd, J = 10.0, 8.2 Hz, 12H), 7.25 (d, J = 9.8 Hz, 8H), 7.21 (d, J = 8.7 Hz, 8H), 7.13 – 7.00 (m, 64H), 2.69 (dt, J = 13.6, 6.8 Hz, 4H), 1.92 (d, J = 11.5 Hz, 24H), 1.10 (d, J = 6.8 Hz, 24H). ^{13}C NMR (151 MHz, CD_2Cl_2) δ 163.40, 155.93, 154.52, 146.37, 144.05, 142.47, 142.11, 141.89, 141.62, 140.61, 132.25, 131.63, 131.55, 131.32, 131.04, 130.71, 130.34, 130.25, 129.91, 129.88, 129.33, 128.83, 128.78, 128.77, 128.21, 128.11, 128.04, 127.00, 126.95, 126.89, 126.24, 126.23, 126.09, 125.71, 125.03, 124.58, 124.56, 124.55, 124.48, 124.47, 122.85, 122.74, 122.54, 119.98, 98.49, 29.48, 24.13, 14.80. HR-MS(MALDI-TOF, m/z): calculated for $C_{246}H_{166}F_{24}N_2O_8S_8^+$ for $[M+1]^+$ 3989.01, found 3990.55 $[M+1]^+$. HPLC purity: 98.9%.

1.3 CHARACTERIZATIONS AND METHODS

1.3.1 Instruments

^{1}H and ^{13}C NMR spectra were recorded on a 600 MHz Bruker AscendTM spectrometer using $CDCl_3$ or DMSO as solvent and tetramethylsilane as internal standard. High resolution mass spectra (HR-MS) were recorded on a BrukerDaltonics SolariX 7.0T instrument or a MALDI-TOF-TOF (Bruker ultrafleXtreme). The purities were determined by high performance liquid chromatograph (HPLC) system equipped with Waters 1525 Binary HPLC Pump, 5 μm 4.6 mm × 150 mm Spherisorb cyano column and 2489 UV/Visible detector. X-ray diffraction (XRD) spectra were obtained on an X-ray diffractometer system (PANalytical B.V.，Empyrean) with a scanning time of 0.82 s for each step of 2θ = 0.01313°using a Cu anode. UV-vis spectra were recorded using a Shimadzu UV-vis-NIR spectrophotometer (UV-3600). PL spectra were recorded using Edinburgh Instruments (FLS920 spectrometer). The optical storage test and Figure S24-S25 was test on a fluorophotometer (Hitachi F-7000). Considering the influence of stay lights, all the fluorescence data were measured on the condition of adding a 550 nm long wavelength pass filter in the front of sample (**Figure S26**). Due to the low responsivity, high noise and low reliability of the detector (R928) of our spectrofluorometer (FLS920 instrument in Edinburgh) above 800 nm, we did not test the fluorescence spectra after 850 nm. The 302 nm UV light are from a transmission platform (UVP, LMW-20) and 405 nm light from Anfu Electronics Co. Ltd. (510B) LEDs. Visible light comes from a 621 nm LED (3W, Daheng Optics). These photos were taken with a Nikon D90 camera. For the optical

properties measurement, the 302 nm, 405 nm, and 621 nm light power density are 1.87 mW/cm^2, 26.0 mW/cm^2 and 12.8 mW/cm^2, respectively

1.3.2 Preparation of TDI-4(DTE-TPE) samples for testing

Preparation of TDI-4(DTE-TPE) solution: First, TDI-4(DTE-TPE) was dissolved in THF or DCM to prepare a mother liquor with a concentration of 1.0×10^{-3} mol/L. A solution with a concentration of 1.0×10^{-6} mol/L was obtained by injecting 5 μL of the above stock solution into 5 mL of solvents (such as THF, DMF, toluene, hexane).

Preparation of PMMA film doped with TDI-4(DTE-TPE): 100 mg/mL PMMA polymer mother liquor was prepared first. Then, 0.5 mL mother liquor was taken, and 1 mg TDI-4(DTE-TPE) dye was added to result a 2 mg/mL chloroform solution. After ultrasonic dispersion, 100 μL above solution was dropped on the quartz substrate, and then rotated at 400 rpm for 5 s followed by 3000 rpm for 40 s to given a PMMA polymer film doped with 2 wt% dye.

1.3.3 UV-Vis Absorption and Fluorescence Spectroscopy (FL) Measurements

The absorption and fluorescence Spectra of TDI-4(DTE-TPE) in THF solution (C = 1.0×10^{-6} mol/L) and in PMMA film (both concentration of 2 wt %) were obtained at room temperature using Shimadzu UV-vis-NIR spectrophotometer (UV-3600) and Edinburgh's FLS920 spectrometer, respectively. For the photocyclization reaction, absorption and FL spectra were measured after exposure to 302 nm or 405 nm light (8 mW/cm^2) for various times until the photostationary state were reached (absorption no longer changed under continuous 405 nm illumination). For the photocycloreversion reaction, the absorption and FL spectra were recorded during different time periods of irradiation of the above PSS samples with 621 nm light.

1.3.4 Aging testing

The aging test was conducted on an constant temperature and humidity testing machine (NK-TOPH-30-C) at control temperature of 85 °C and relative humidity of 85 % in the air atmosphere. The test sample was the open-from and photostationary state TDI-4(DTE-TPE) PMMA film (2 wt%). The photostationary state sample was achieved by full 405 nm irradiation on the open form sample. The absorption spectra were test at different aging test time to evaluate the durability of samples

1.3.5 Photoisomerization quantum yield measurement

The UV-Vis absorption spectrum changes of compound TDI-4(DTE-TPE) in THF (1.0×10^{-6} mol/L) under 405 nm or 302 nm light irradiation were monitored until the photostationary state was reached. Then, the above sample was irradiated with 621 nm visible light, and the absorption spectra at different times were recorded. The light power densities at 302 nm, 405 nm and 621 nm was measured using a Newport photometer. The absorbance values of TDI-4(DTE-TPE) at 608 nm were fitted by a single exponential function (**Figure S10**). Estimation of photoisomerization quantum yields was performed according to standard methods and formulas from previous work. [1]

1.3.6 The fluorescence quantum yield measurement

The relative fluorescence quantum yields Φ_F were measured with the fluorescence quantum yield of TDI (Φ_F = 0.9 in chloroform) as reference.[3, 4] The relative fluorescence quantum yields of an unknown compound (Φ_u) was determined by a standard method and through the following formulas:

$$\Phi_u=\Phi_s*(F_u/F_s)*(A_s/A_u)*(n_u/n_s)^2$$

Where Φ is relative fluorescence quantum yield, F is the integrate area value of fluorescence spectra, A is the absorbance at excitation wavelength, n is the refractive index of solvent, u means unknown product; s means standard dye.

1.3.7 Simulation Calculation of Density Functional Theory (DFT)

DFT calculations were performed with Gaussian 09 package, revision A.02.[5] Molecule structures were first pre-optimized with MM2 minimize energy optimization by Chem 3D software and then the optimized structure with removed lone pair electrons was input into the Gaussian 09 for calculation. The Becker's three-parameter exchange functional[6] along with the Lee Yang Parr's correlation functional[7] (B3LYP) that can well predict the geometric structures of organic molecules, was adopted to optimize the ground state geometries of all molecules in assistant with the 6-31G(d) basis set in gas phase at temperature of 298.15 K. [8]

2 OPTICAL PROPERTIES AND OTHER CHARACTERIZATION RESULTS

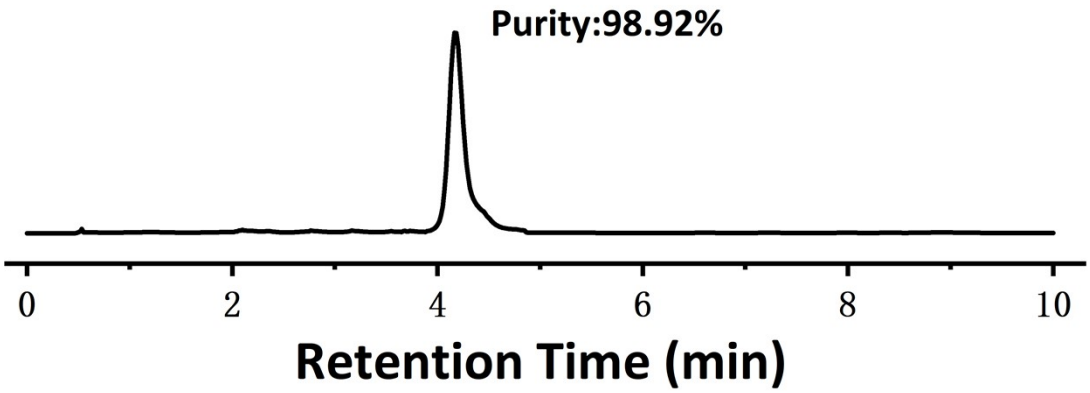

Figure S1 The HPLC curves of TDI-4(DTE-TPE). Eluant: 60% dichloromethane in hexane.

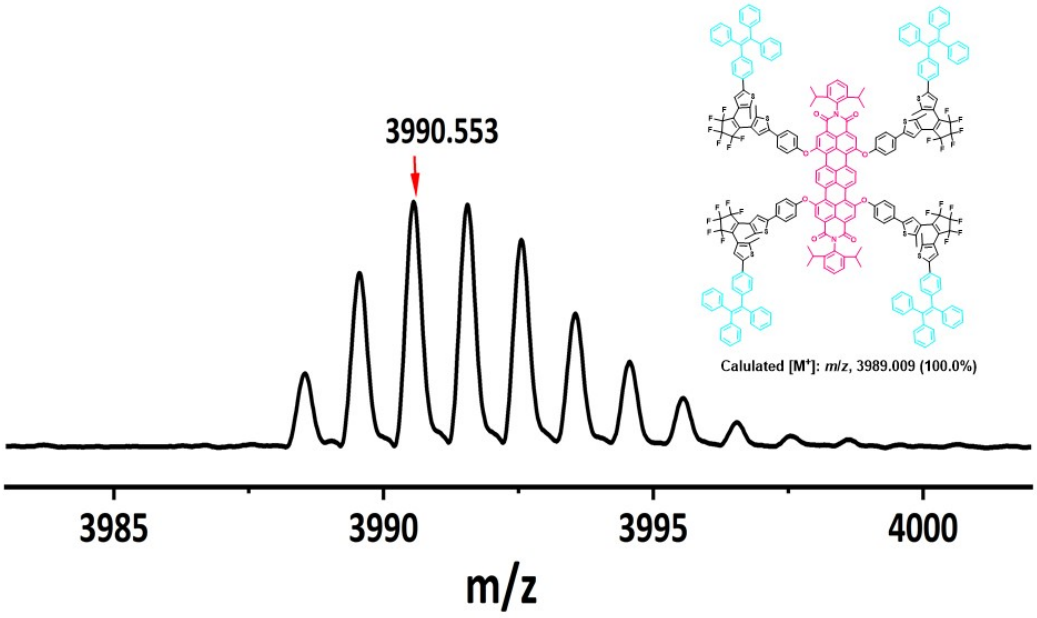

Figure S2 High-resolution mass spectrum of TDI-4(DTE-TPE).

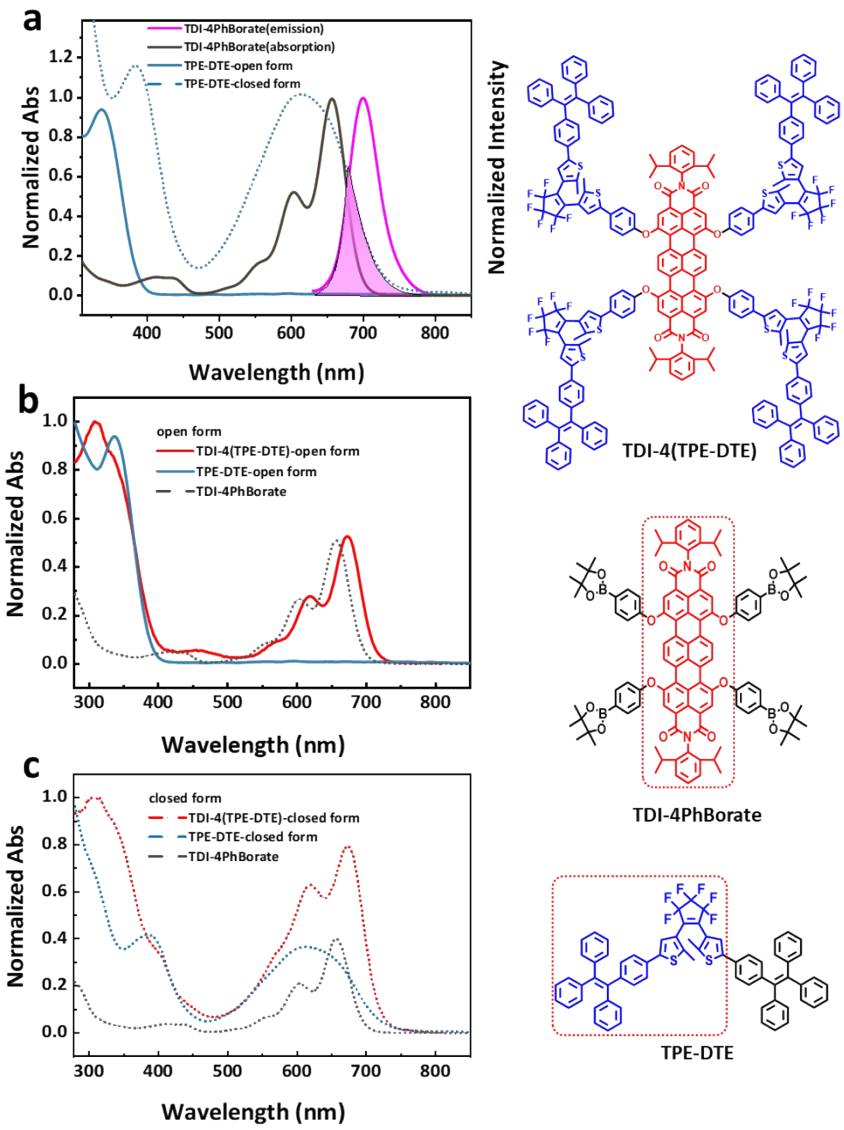

Figure S3 The absorption spectra of TPE-DTE[9] (The model of DTE-TPE groups in TDI-4(DTE-TPE), TDI-4PhBorate (The model of TDI core in TDI-4(DTE-TPE) and TDI-4(DTE-TPE). The molecular structures of the model compounds and TDI-4(DTE-TPE) are listed in the right side. (a) The green line and blue line are the absorption spectra of model compound TPE-DTE-o (open form TPE-DTE-TPE) and TPE-DTE-TPE-c (closed form TPE-DTE), respectively. The gray line is the absorption spectra of model compound TDI-O-4PhBorate. The red line is the emission spectra of model compound TDI-O-4PhBorate. The DTE is at (b) open form and (c) closed form states in both model compounds and TDI-4(DTE-TPE). The results indicate that the absorption spectra of TDI-4(DTE-TPE) resembles the addition of that of TPE-DTE moiety model and TDI moiety model.

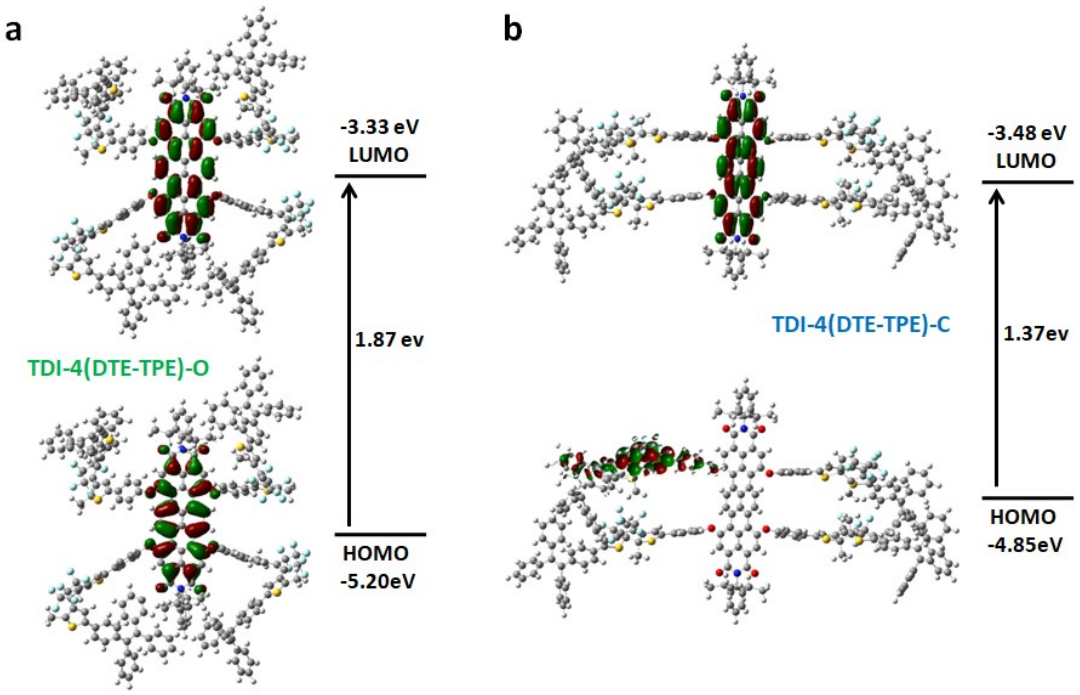

Figure S4 The frontier molecular orbital diagram of TDI-4(DTE-TPE) in open form and closed form calculated using the B3LYP/6-31G(d) basis set. Left: The energy gap value of HOMO-LUMO in open form. Right: The energy gap value of HOMO-LUMO in closed form.

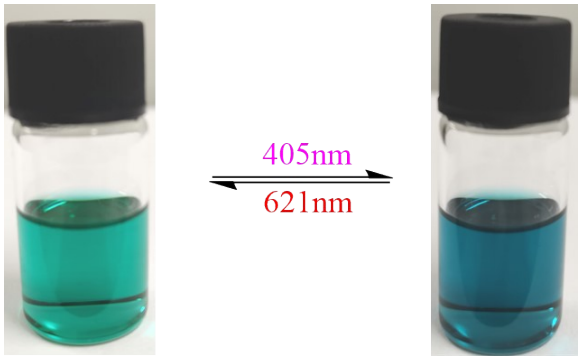

Figure S5 The color change of TDI-4(DTE-TPE) in THF upon 405 nm and 621 nm light irradiations. The concentration is 1×10^{-5} M.

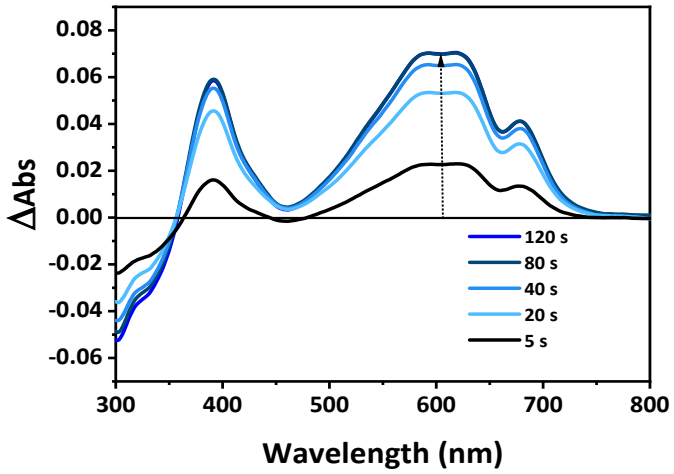

Figure S6 The absorbance changes contributed by the generated closed form DTE moiety in TDI-4(DTE-TPE) which was calculated by subtracting the spectrum at different 405 nm irradiation times with the initial spectrum (open form) in Figure 1 in the main text.

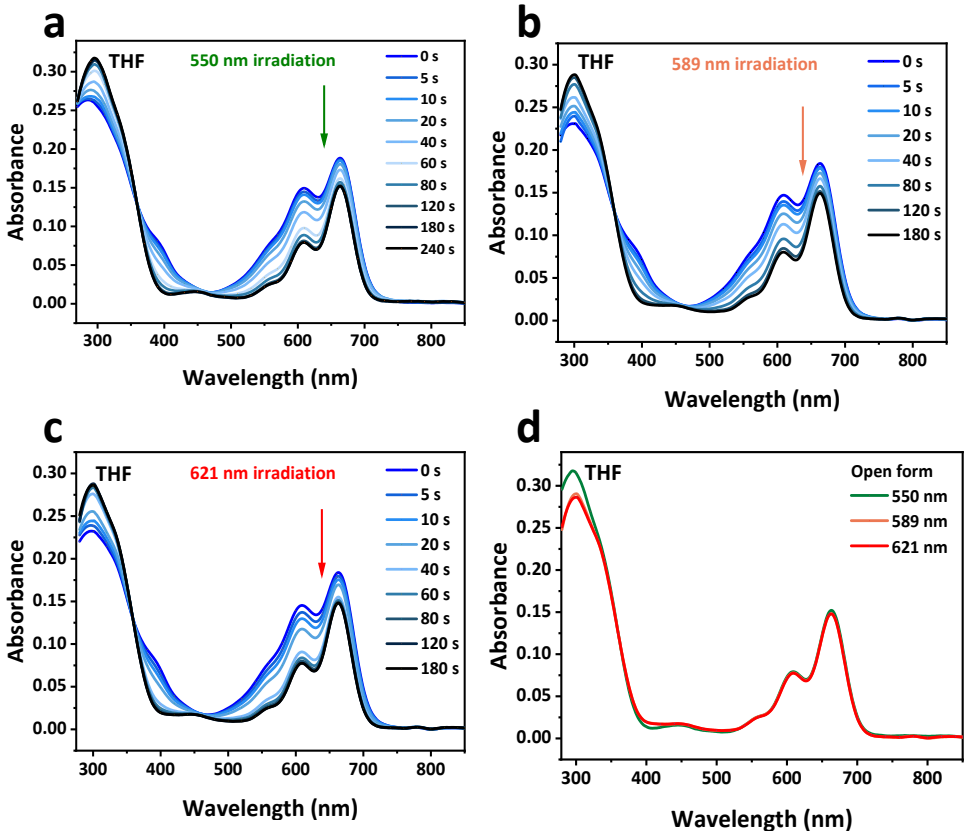

Figure S7 The absorption spectra changes during the photocycloreversion reaction of TDI-4(DTE-TPE)-pss at 405 nm in THF solution (1×10^{-6} M) upon (a) 550 nm, (b)589 nm and (c) 621 nm irradiation and (d) the overlapped final states of (a), (b) and (c). The highly overlap of final states indicate the arrival of the same open form state of TDI-4(DTE-TPE)-o.

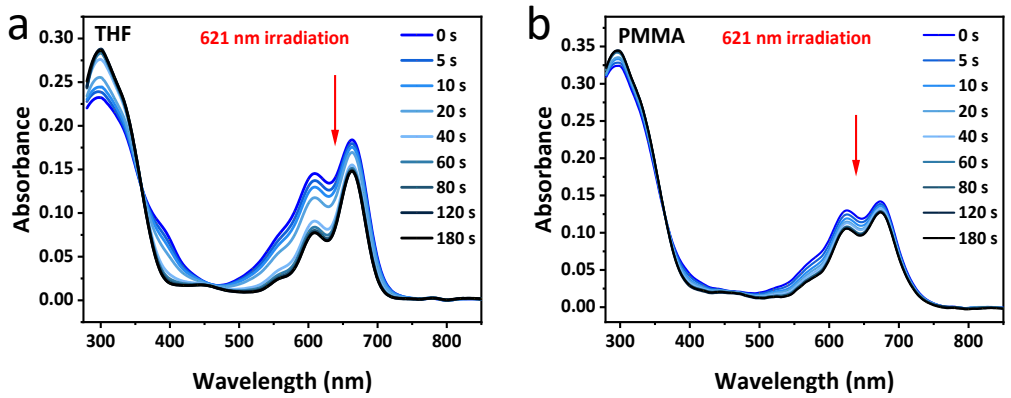

Figure S8 The absorption spectra changes during the photocycloreversion reaction of TDI-4(DTE-TPE)-pss at 405 nm in (a)THF solution (1×10^{-6} M) and (b)PMMA film (2 wt%) under 621 nm irradiations.

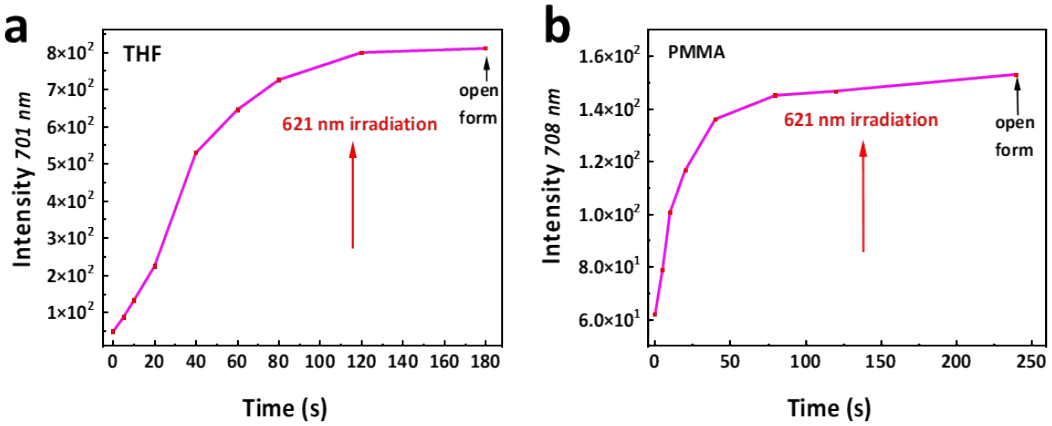

Figure S9 The fluorescence intensity changes during the photocycloreversion reaction of TDI-4(DTE-TPE)-pss at 405 nm in (a) THF solution (1×10^{-6} M) and (b) PMMA film (2 wt%) under 621 nm irradiation. The excitation wavelength is 600 nm, the monitored fluorescence wavelengths are 701 nm and 708 nm for the THF solution and PMMA film samples, respectively. The fluorescence intensity did not increase anymore and reached a plateau just synchronously with the absorption spectra changes in **Figure S8**, which indicates the arrival of open form state.

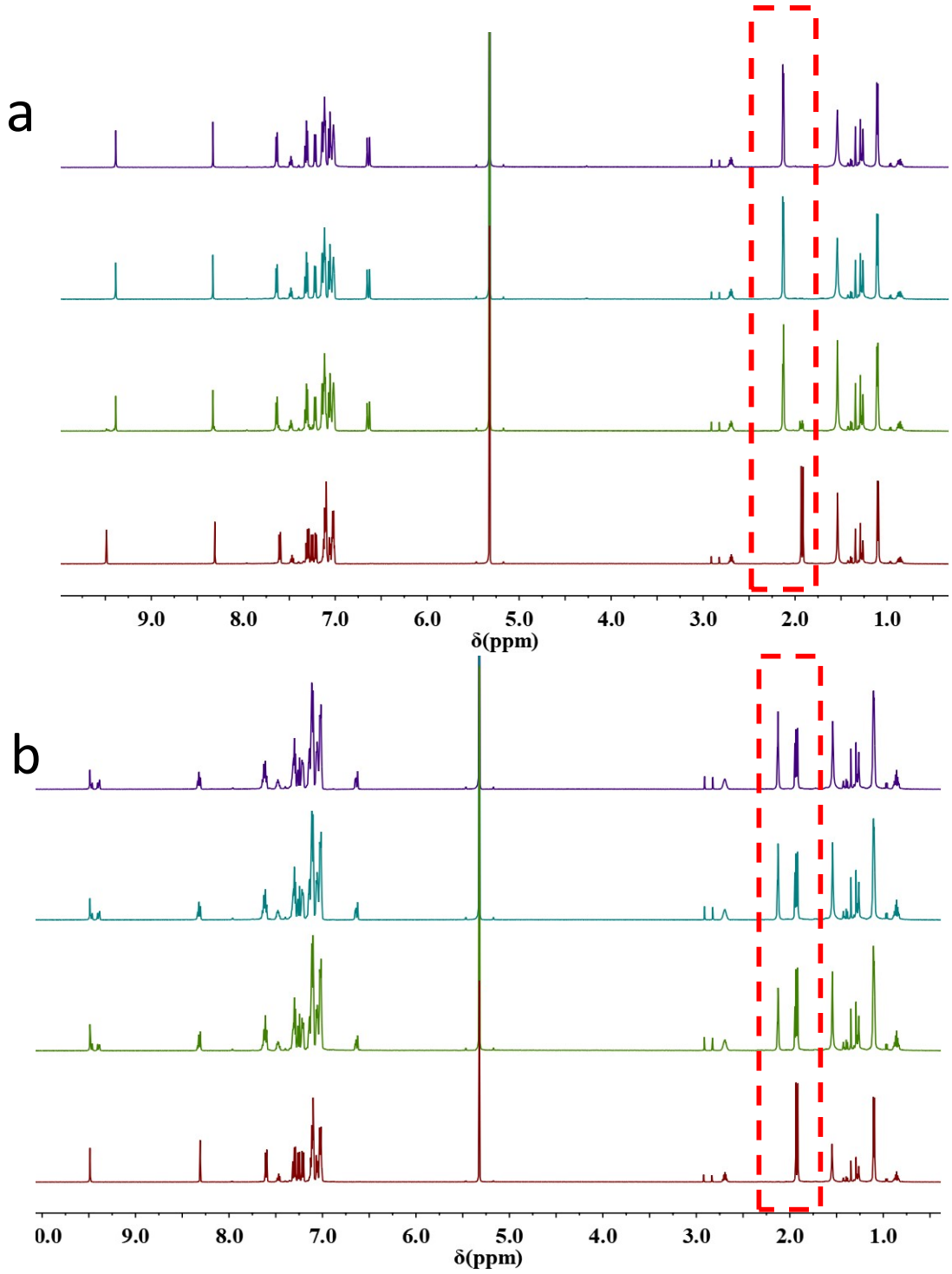

Figure S10 The photoisomerization process monitored by ^{1}H NMR upon (a) 302 nm irradiation and (b) 405 nm irradiation. Solvent: CD_2Cl_2. Concentration: 2.5 mg/mL. The red box shows the peak of the $–CH_3$ groups on the thiophene rings of open form and closed form TDI-4(DTE-TPE).

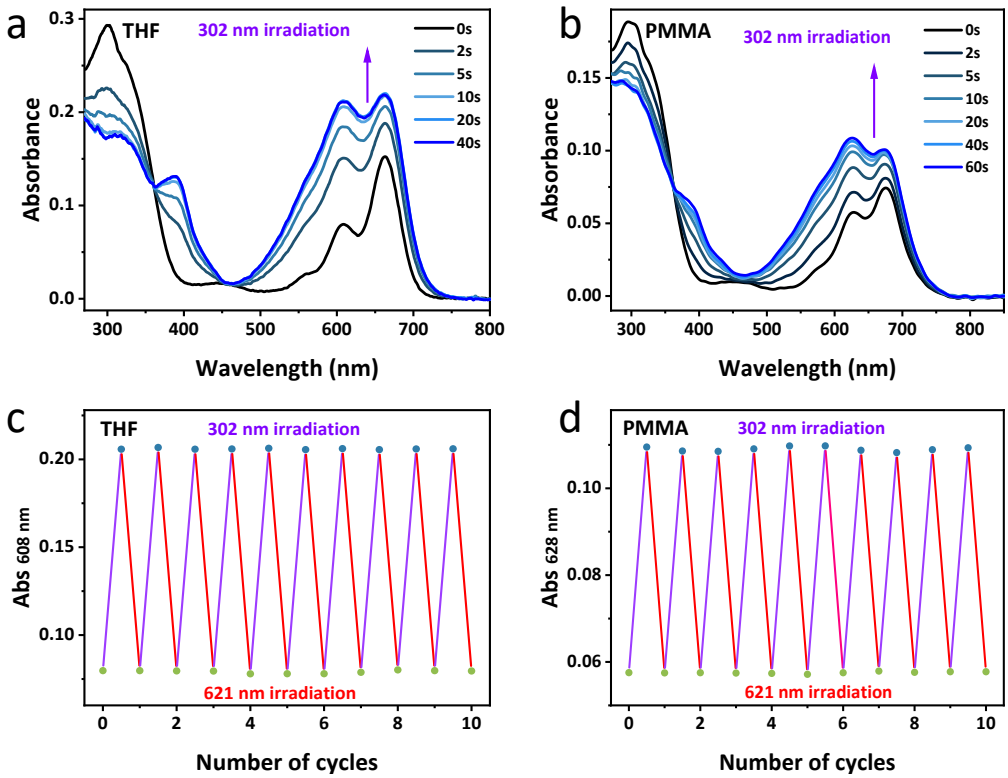

Figure S11 Absorption spectra changes of TDI-4(DTE-TPE) in (a) THF solution (1×10^{-6} M) and (b) PMMA film (2 wt%) upon 302 nm ultraviolet light irradiation. (c) Photoswitching cycles of absorbance at 608 nm of TDI-4(DTE-TPE) in THF solution under alternating irradiations of 302 nm UV light (10 s) and 621 nm red light (5 min). (d) Photoswitching cycles of absorbance at 628 nm of TDI-4 (DTE-TPE) PMMA film under alternating irradiation of 302 nm UV light (20 s) and 621 nm red light (8 min).

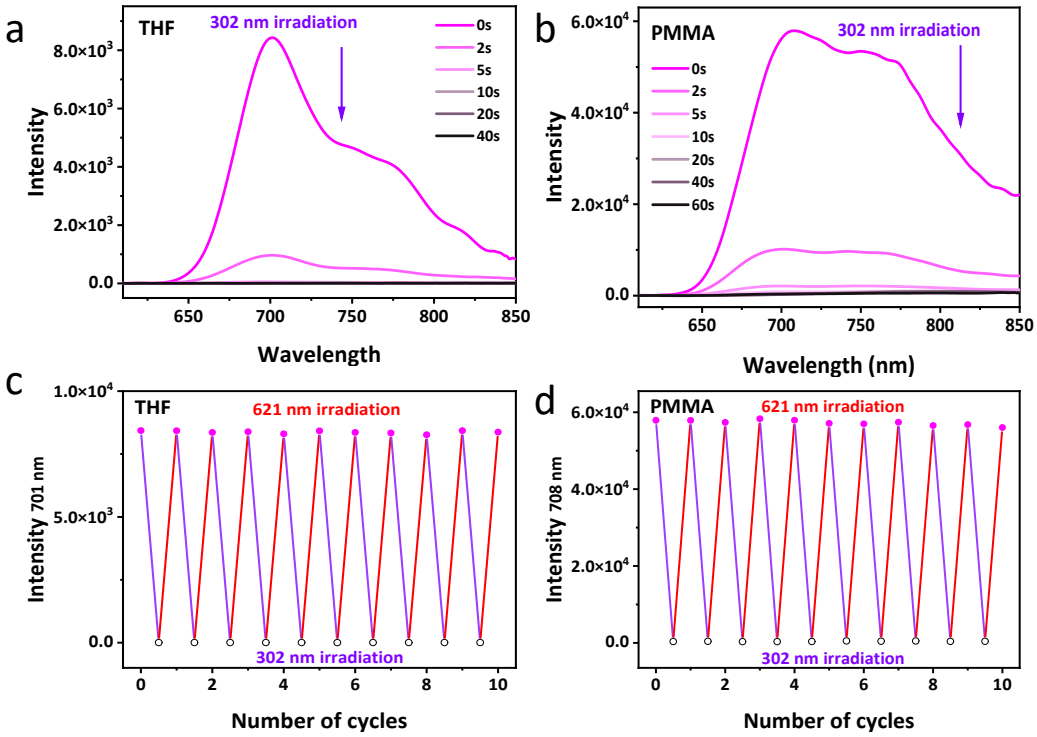

Figure S12 Fluorescence spectra changes of TDI-4(DTE-TPE) in (a) THF solution and (b) PMMA film (2 wt%) upon 302 nm UV light irradiation. (c) Photoswitching cycles of fluorescence intensity at 701 nm of TDI-4(DTE-TPE) in THF solution under alternating irradiation of under alternating irradiations of 302 nm UV light (10 s) and 621 nm red light (5 min). (d) Photoswitching cycles of fluorescence intensity at 708 nm of TDI-4(DTE-TPE) PMMA film under alternating irradiation of 302 nm UV light (20 s) and 621 nm red light (8 min). The fluorescence excitation wavelength is 600 nm.

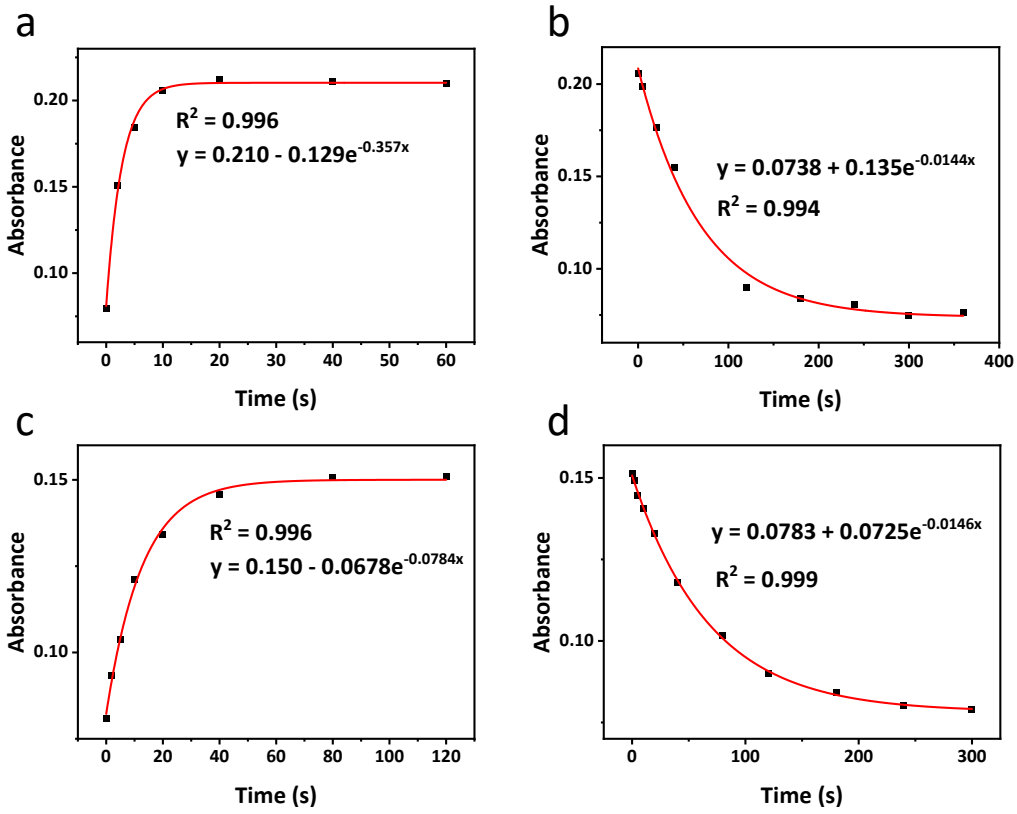

Figure S13 The photoisomerization dynamics of TDI-4(DTE-TPE). The absorbance at 608 nm of TDI-4(DTE-TPE) in THF solution varied with the irradiation time of (a) 302 nm UV light to arrive a photostationary state followed by (d) 621 nm red light irradiation. The absorbance at 608 nm of TDI-4(DTE-TPE) in THF solution varied with the irradiation time of (a) 405 nm visible light to arrive a photostationary state followed by (d) 621 nm red light irradiation. The concentration is 1×10^{-6} M. The fitting curves (red lines) were all fitted well with the single exponential functions (coefficient correlation $R^2 > 0.993$). It indicated the fact of first-order reaction of the photocyclization.

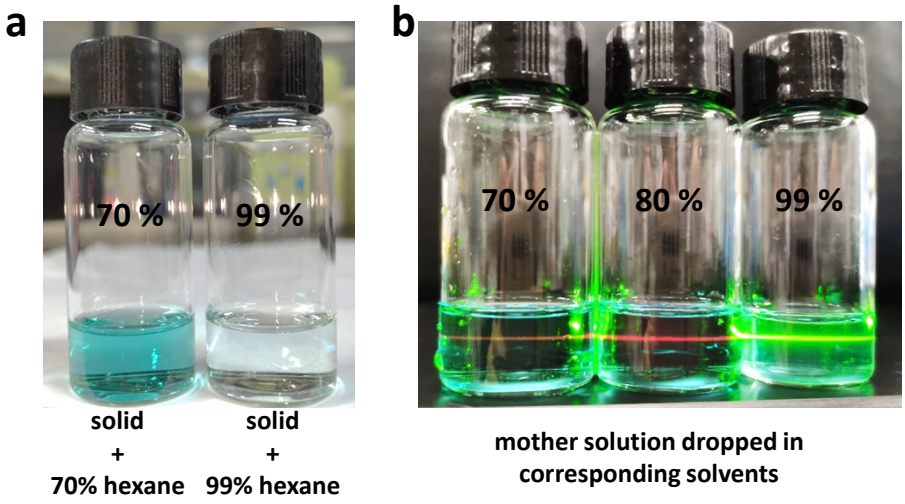

Figure S14 (a) The left side is the mixture prepared by mixing 70 % hexane in DCM with the TDI-4(DTE-TPE) solid sample, while the right side is the mixture prepared by mixing 99 % hexane in DCM with the TDI-4(DTE-TPE) solid sample. The result shows that TDI-4(DTE-TPE) can dissolve in 70 % hexane in DCM but not the 99 % hexane in DCM. (b) The Tyndall effect test result of the TDI-4(DTE-TPE) in hexane DCM-hexane binary solvent with different volume fraction of hexane by a green laser. The concentrations are both 5×10^{-6} M. There is a strong Tyndall effect in the 99% hexane sample, meaning the formation of aggregation particles. The red light in 70 % and 80% hexane is the fluorescence from the solution after absorbed the green light, showing negligible scattering of green light (Tyndall effect)

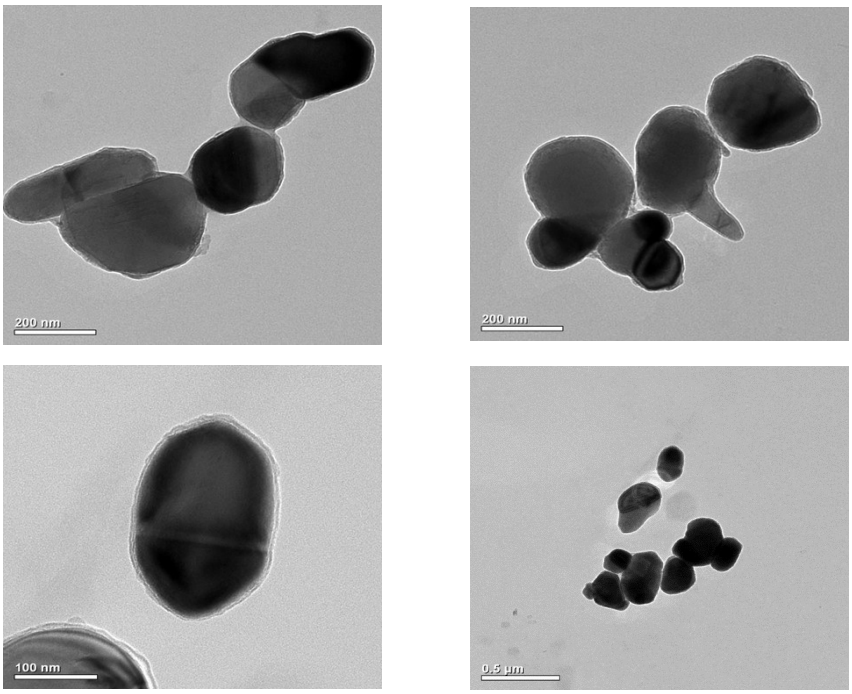

Figure S15 The TEM morphology of TDI-4(DTE-TPE) nanoparticles formed in 99% hexane in DCM.

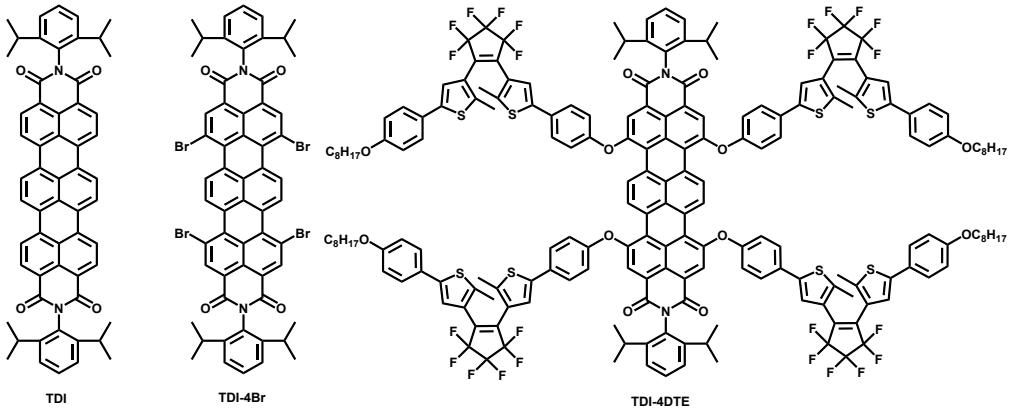

Figure S16 Molecular structures of TDI, TDI-4Br and TDI-4DTE (which are from our previous work[2]), respectively. The TDI-4DTE has the soft C_8H_{17}-O-groups which is less bulky then propeller-shape TPE groups in TDI-4(DTE-TPE).

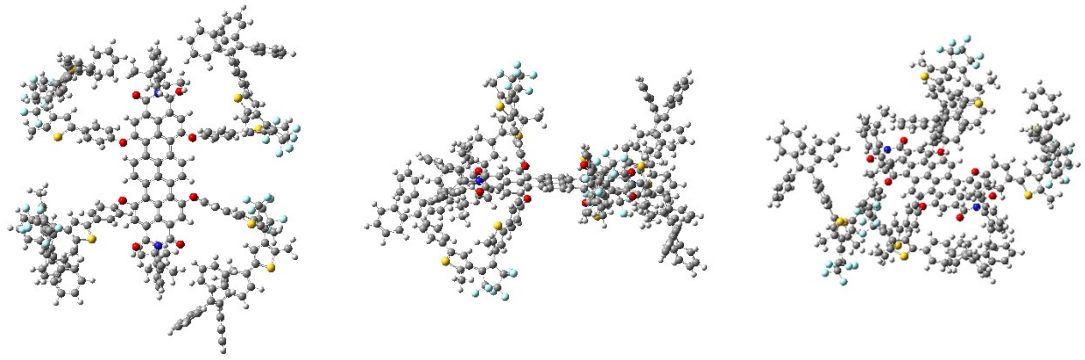

Figure S17 The optimized electronic structure of TDI-4(DTE-TPE) molecules with different viewing angles showing a bulky three-dimensional conformation where the TPE-DTE group wrapped the TDI core.

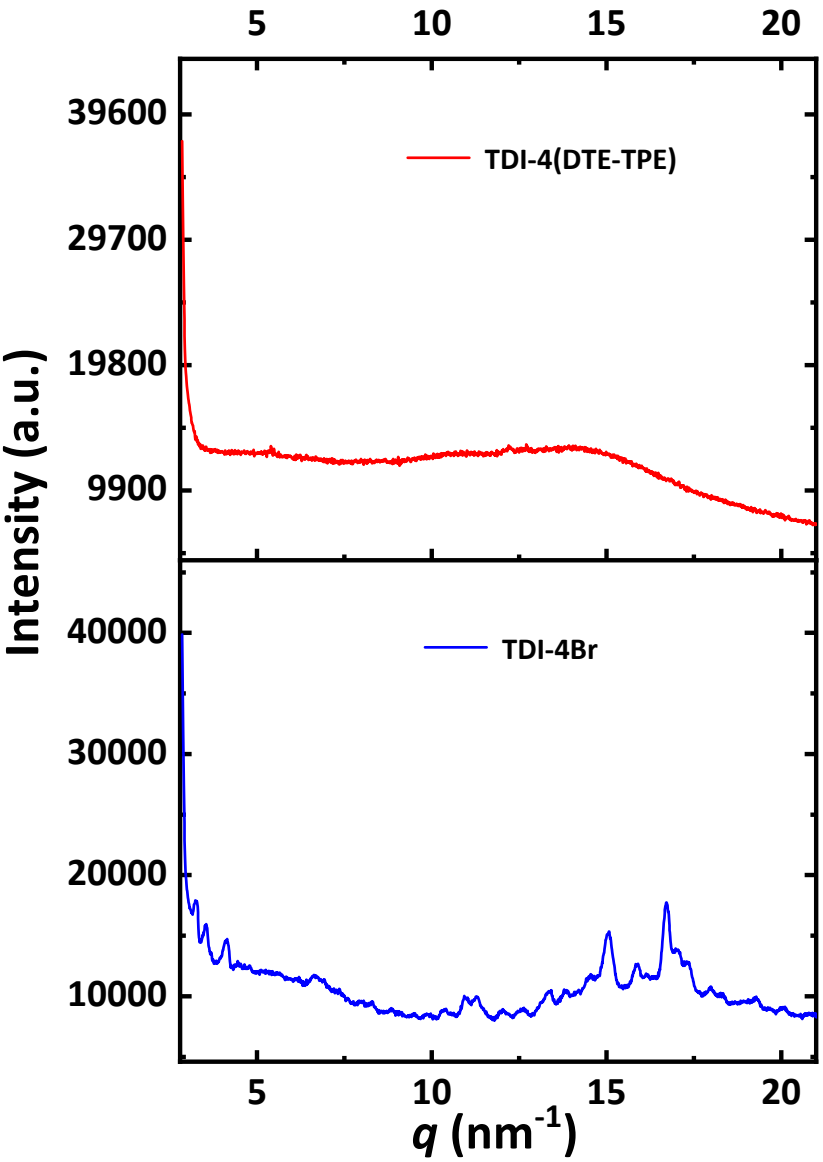

Figure S18 The X-ray diffractogram of TDI-4(TPE-DTE) (red) and TDI-4Br (blue). TDI-4(TPE-DTE) powder is prone to be an amorphous state indicating the large substituents impairing the orderly stacking ability. TDI-4Br has obvious XRD peaks indicating the tendency of crystallization. The dominant reflexes at q = 15−20 nm^{-1} were interpreted as the interplanar distance referencing the literatures.[10] The interpanar distance of TDI-4Br molecules in power state is about 3.76 Å.

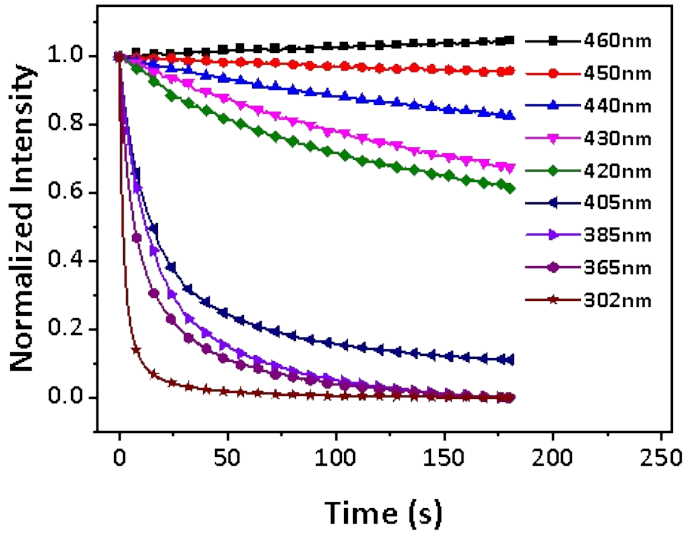

Figure S19 The normalized fluorescence intensity (the intensity *I* divided by the initial intensity I_0) at 708 nm decays of TDI-4(DTE-TPE) PMMA film upon 302~460 nm irradiations. The irradiation lights also play the role of excitation lights from the fluorescence spectrophotometer itself. The result indicated that the photocyclization of TDI-4(DTE-TPE) has a considerable sensitivity on visible light above 405 nm wavelength.

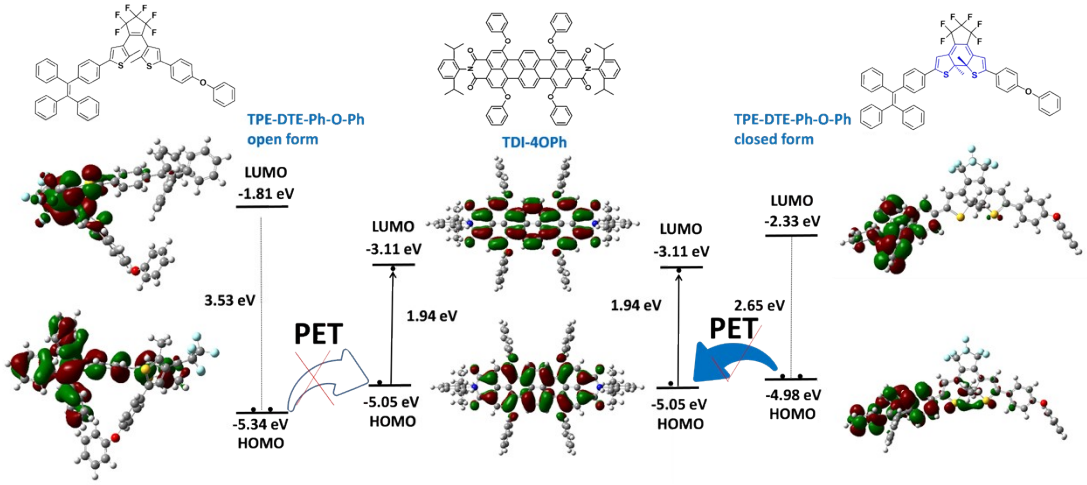

Figure S20 The frontier molecular orbital (LUOM, HOMO as well as the energy gaps) diagram of the model compounds of the moieties in the TDI-4(DTE-TPE) calculated using the B3LYP/6-31G(d) basis set. The TPE-DTE-Ph-OPh is the model compound of diarylethene moiety in TDI-4(DTE-TPE), while TDI-4OPh represents the model of DTE unit.

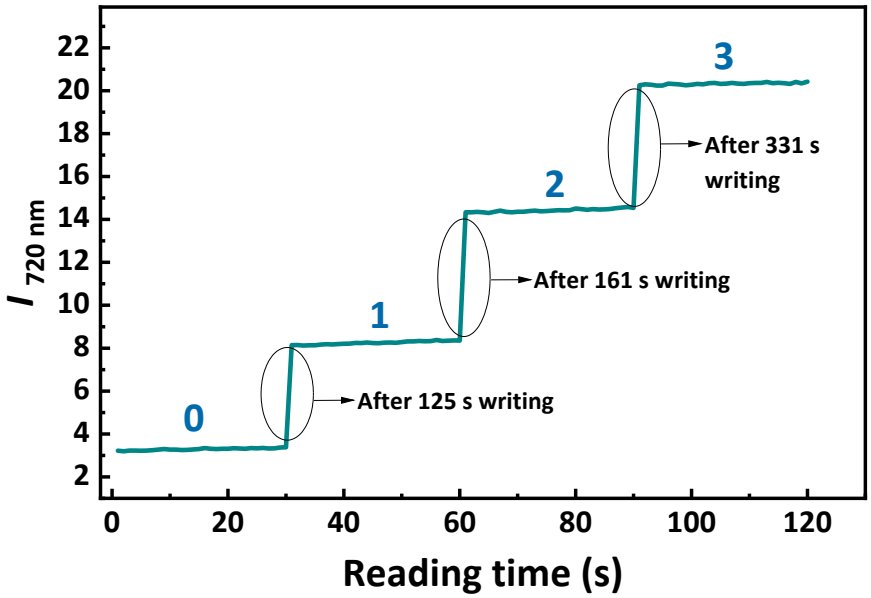

Figure S21 Four-level storage model of TDI-4(DTE-TPE) PMMA film. The film was irradiated with 405 nm light to achieve the dark state. Then, the information (with the form of fluorescence intensity at 720 nm) was recorded with given exposure times (125 s, 161 s, and 331 s respectively) of 589 nm light (writing) to achieve linear four stages optical storage. The fluorescence intensity at 720 nm was continuously read out for 30 s upon 680 nm excitation (reading) for each stage.

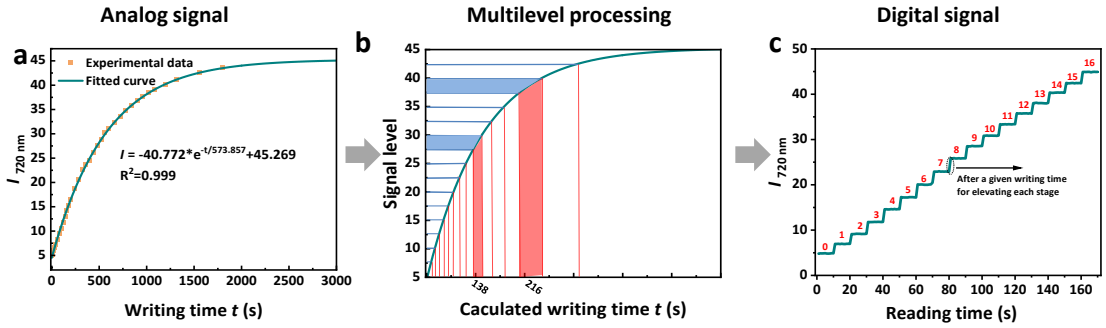

Figure S22 The 16-level optical storage model of TDI-4(DTE-TPE) PMMA film. (a) The fluorescence intensity of TDI-4(DTE-TPE)'s PMMA Film varied with the exposure time of the writing light (621 nm). The experiment data was fitted well with a single exponential function. The curve looks like a nonlinear analog signal. (b) The signal amplitude in the variation curve of (a) was divide into 16 linear levels to figure out the corresponding times of writing time for each level of signal. (c) After irradiating for the given exposure times of wring light according to (a), linear 16 levels of signal (NIR) fluorescence at 720 nm) were achieved and read out by a reading light (680 nm).

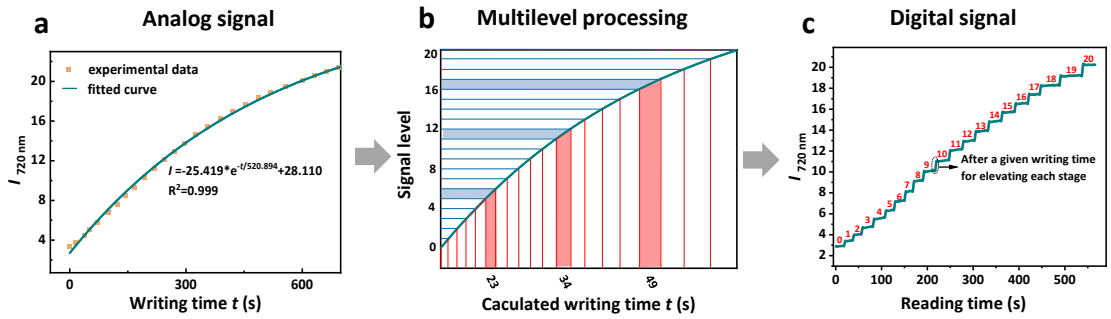

Figure S23 The 20-level optical storage model of TDI-4(DTE-TPE) PMMA film. (a) The fluorescence intensity of TDI-4(DTE-TPE) PMMA Film varied with the exposure time of a writing light (589 nm). The experiment data was fitted well with a single exponential function. The curve looks like a nonlinear analog signal. (b) The signal amplitude in the variation curve of (a) was divide into 20 linear levels to figure out the corresponding times of writing time for each level of signal. (c) After irradiating for the given exposure times of wring light according to (a), linear 20 levels of signal (NIR)fluorescence at 720 nm) were achieved and read out by a reading light (680 nm).

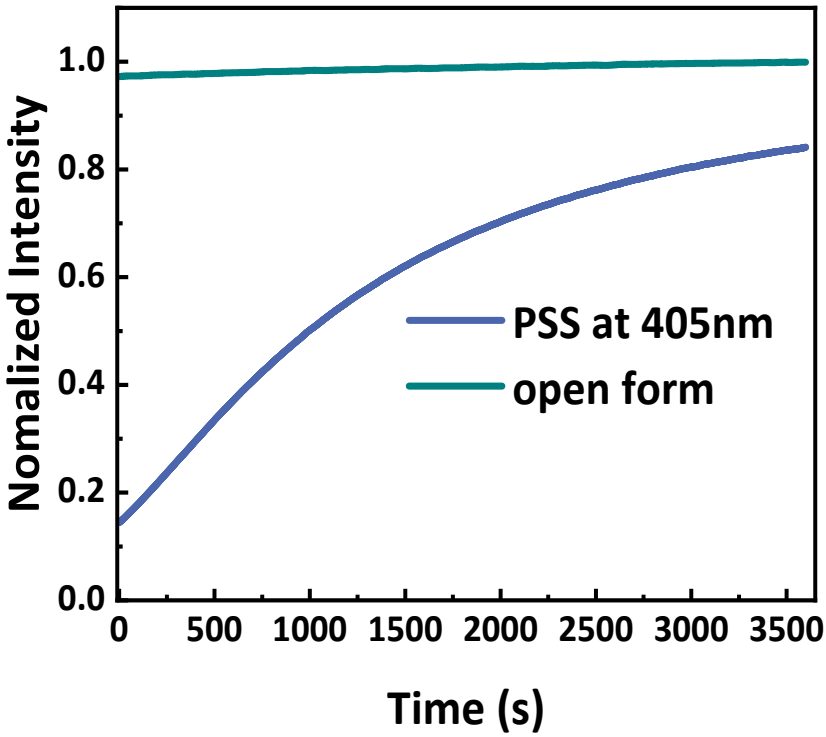

Figure S24 Time-dependent normalized fluorescent intensity at 720 nm of TDI-4(DTE-TPE)-o and TDI-4(DTE-TPE)-pss (405 nm) in PMMA film upon continuing excitation with monochromatic light at 680 nm. The result shows that the read-out process of the fluorescence is a destructive manner.

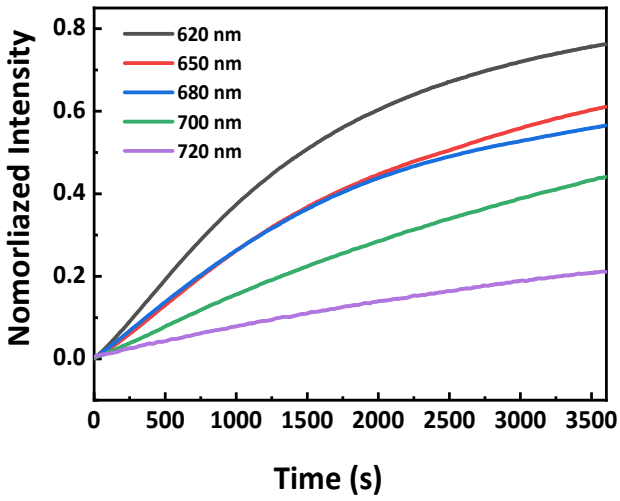

Figure S25 Time-dependent normalized fluorescence intensity of TDI-4(DTE-TPE)-pss (405 nm irradition) in PMMA film upon continuing excitation with monochromatic lights at 620 nm, 650 nm, 680 nm,700 nm and 720 nm. The detection wavelength was 720 nm when the excitation wavelength was 620 nm, 650 nm or 680 nm. The detection wavelength was 750 nm when the excitation wavelength was 700 nm or 720 nm. Normalization of the fluorescence intensity upon each irradiation was conducted by setting the fluorescence intensity of TDI-4(DTE-TPE)-pss as 0 and the fluorescence intensity of TDI-4(DTE-TPE)-o as 1 at the corresponding irradiation wavelength.

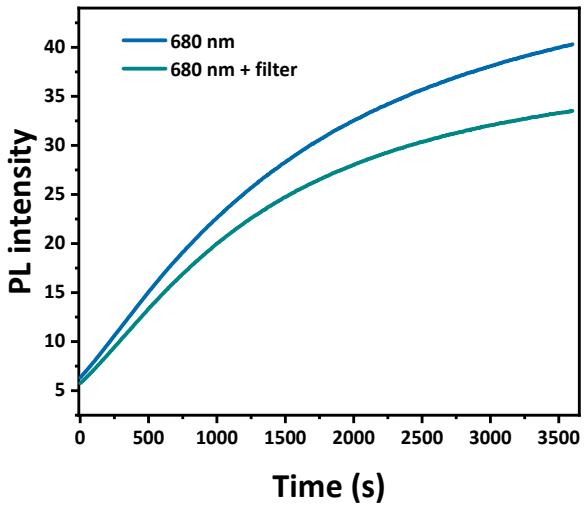

Figure S26 Time-dependent normalized fluorescent intensity at 720 nm of TDI-4(DTE-TPE)-pss (405 nm) in PMMA film upon continuing excitation with and without a long pass filter (pass through > 550). The filter will reduce the influence of the short wavelength stray lights. It will also attenuate the irradiation intensity in some degree and therefore a slight slower photocycloreversion reaction is exhibited.

Table S1 Fluorescence quantum yield Φ_F of TDI-4(DTE-TPE) in different solvents

Parameter	99% hexane[a]	Cyclo-hexane	toluene	THF	chloroform	DCM	DMF
λ_{em} (nm)	691	682	706	701	715	716	723
Φ_F	0.35	0.52	0.46	0.28	0.24	0.19	0.04

[a] Aggregation state. Φ_F present the relative fluorescence quantum yields which were measured taking TDI in chloroform ($\Phi_F = 0.9$) as the reference.

Table S2 Optical properties of TDI-4(DTE-TPE) in THF and PMMA matrix

Media	Wavelength	λ_{abs} (nm)		λ_{em} (nm)	$R_{on/off}$	FQ
		Open form	Close form			
THF	302 nm	300, 608, 663	390, 609, 663	701	1259	~100%
	405 nm	300, 608, 663	298, 608, 663	701	14	93.6%
PMMA	302 nm	300, 628, 675	295, 628, 675	708	302	~100%
	405 nm	300, 628, 675	300, 628, 675	708	9.5	89.6%

λ_{abs} is the maximum absorption wavelength. λ_{em} is the maximum emission wavelength. FQ is the fluorescence quenching efficiency calculated by dividing the initial intensity at λ_{em} with the intensity at λ_{em} of photostationary state. Fluorescence on/off ratios $R_{on/off}$ were calculated by comparing the intensity at λ_{em} before and after 302 nm and 405 nm irradiation.

3 NMR SPECTRA

TDI-O-4PhBr

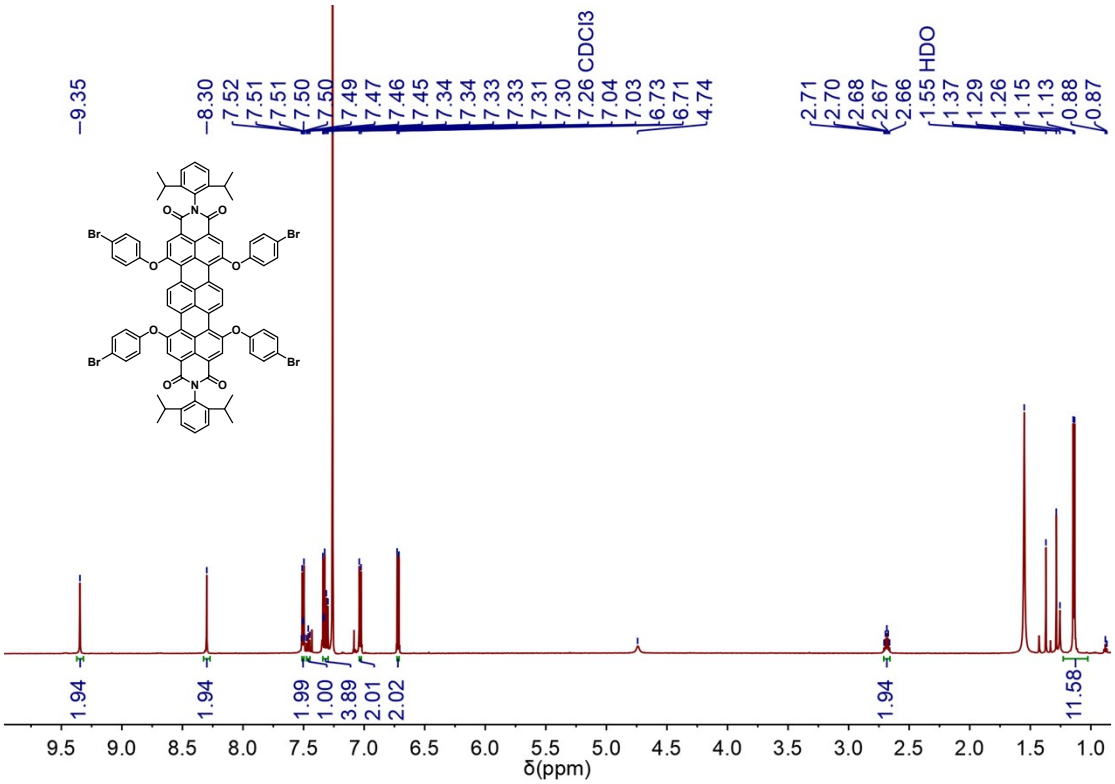

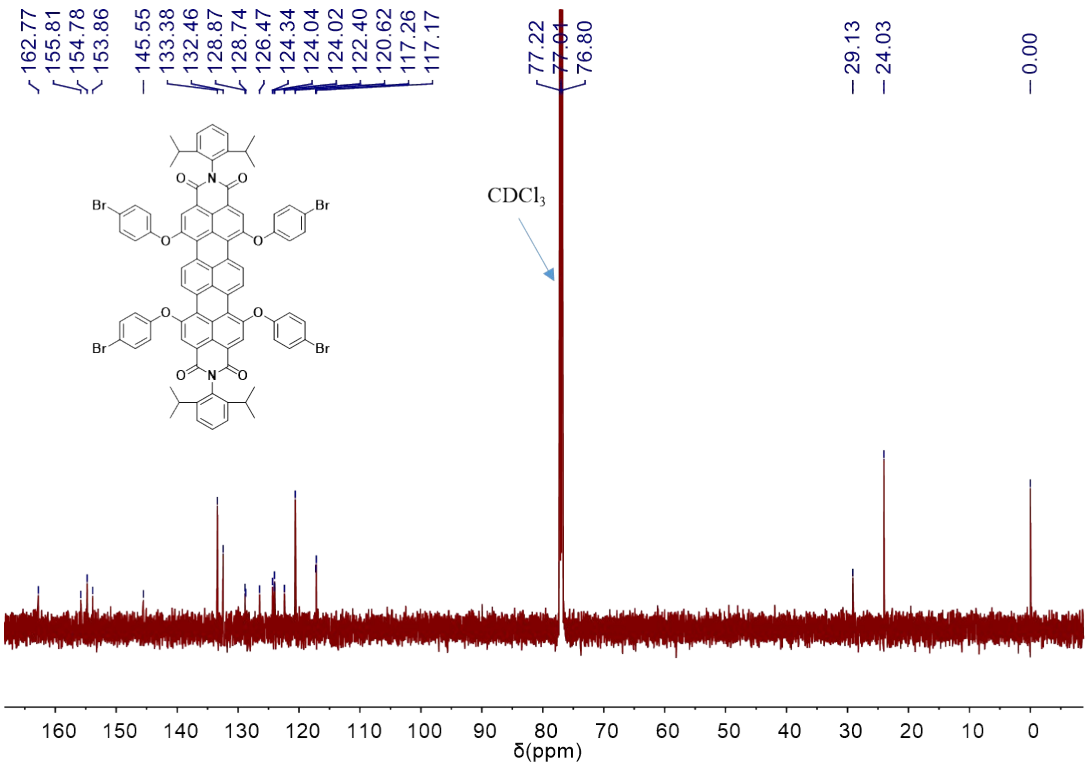

TDI-O-4PhBorate

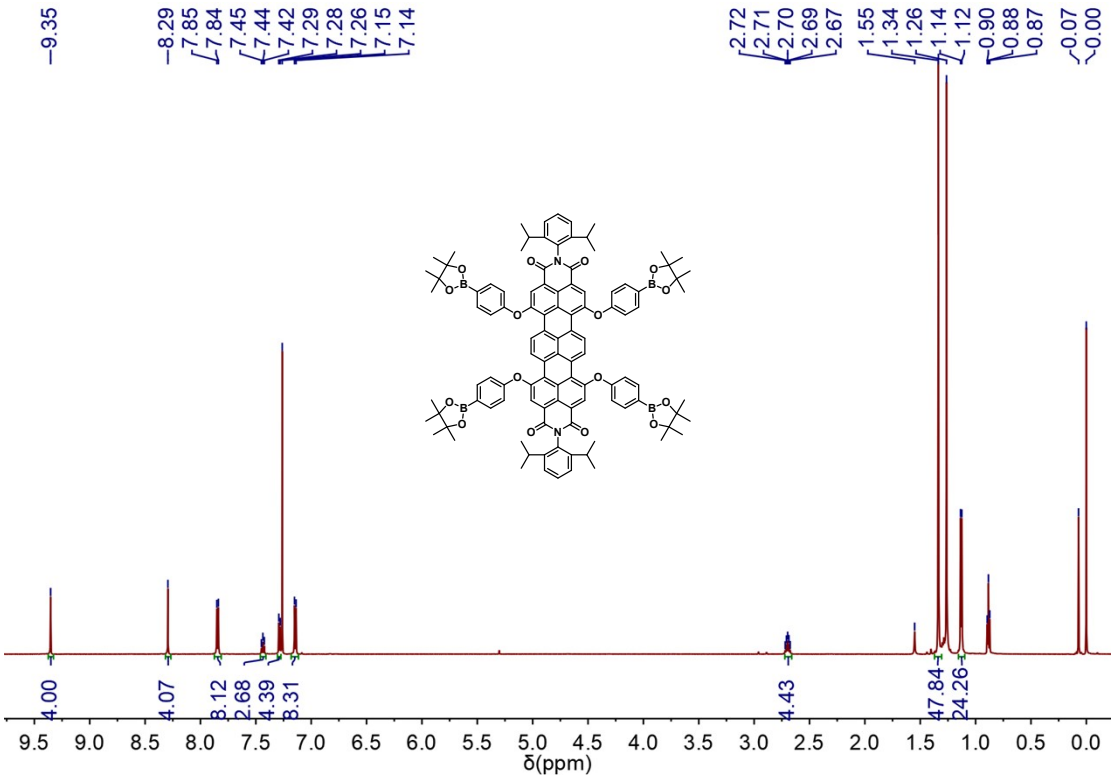

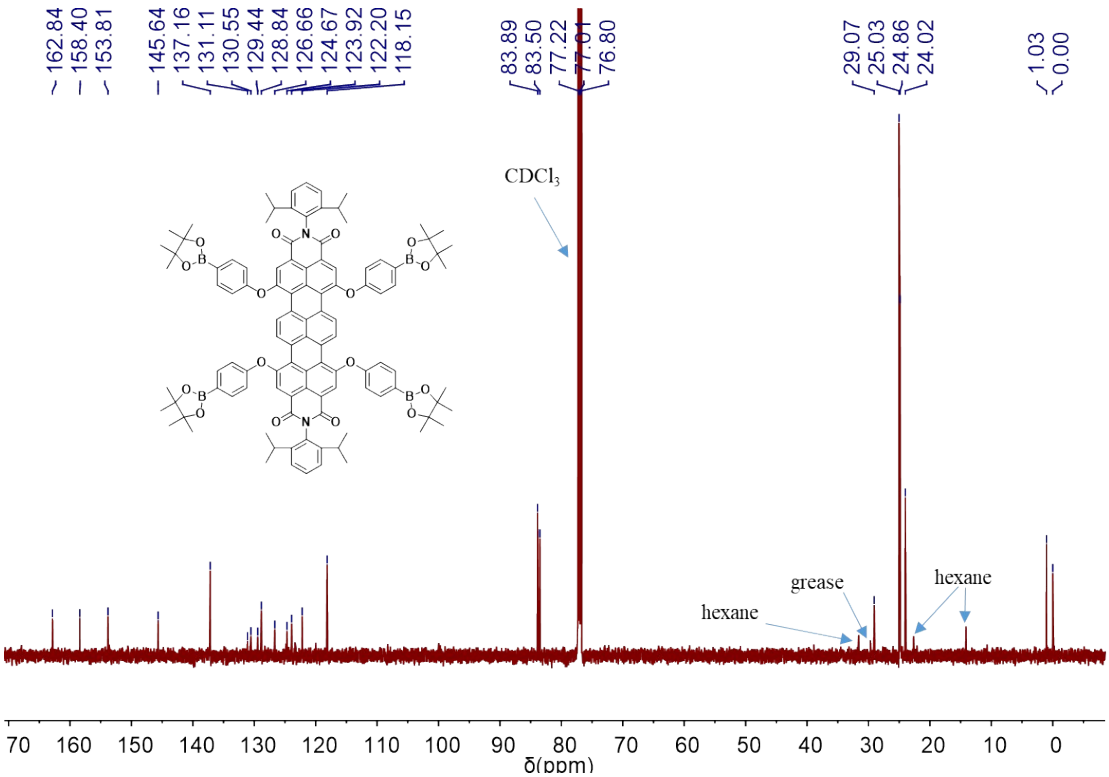

TDI-4(DTE-TPE)

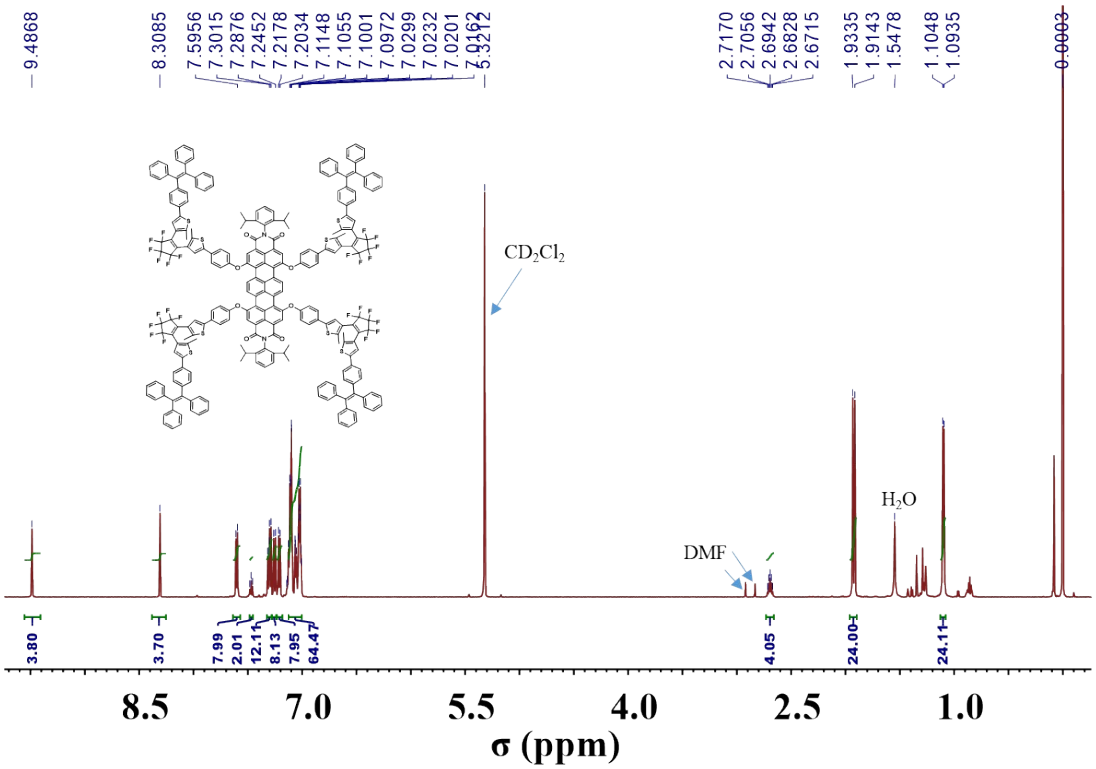
9.4868
8.3085
7.5956
7.3015
7.2876
7.2452
7.2178
7.2034
7.1148
7.1055
7.1001
7.0972
7.0299
7.0232
7.0201
5.3212
2.7170
2.7056
2.6942
2.6828
2.6715
1.9335
1.9143
1.5478
1.1048
1.0935
0.0003
CD2Cl2
H2O
DMF
3.80
3.70
7.99
2.01
12.11
8.13
7.95
64.47
4.05
24.00
24.11
8.5
7.0
5.5
4.0
2.5
1.0
σ (ppm)

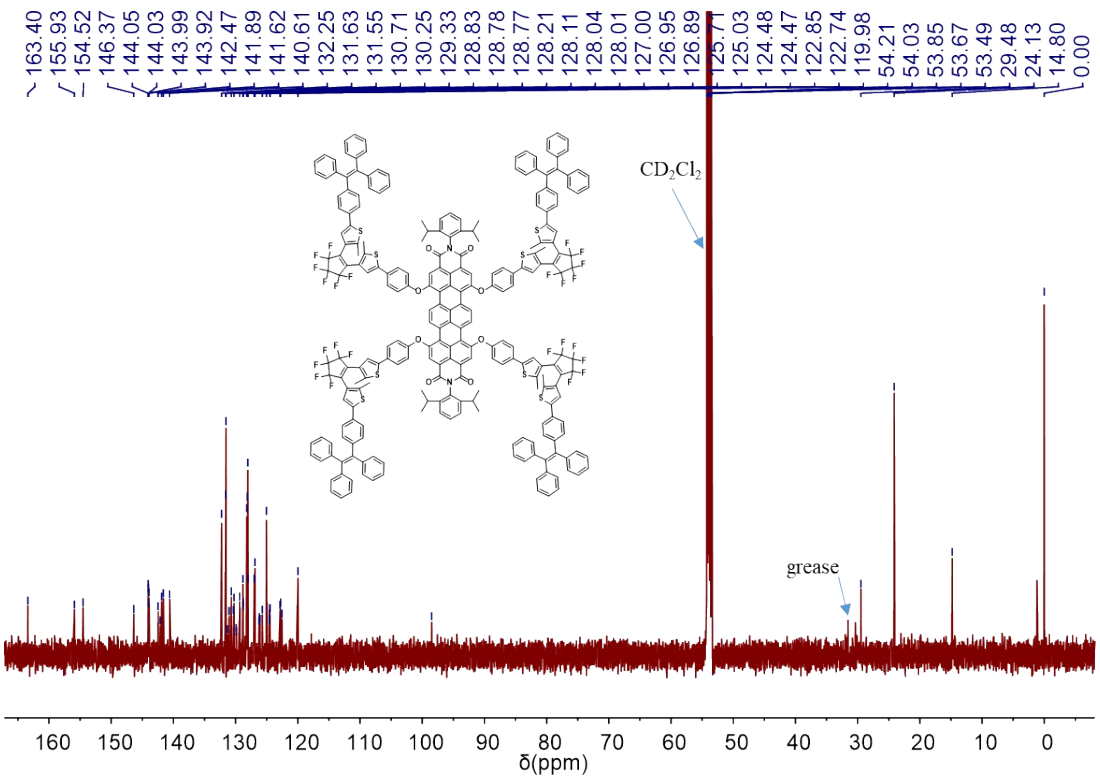
163.40
155.93
154.52
146.37
144.05
144.03
143.99
143.92
142.47
141.89
141.62
140.61
132.25
131.63
131.55
130.71
130.25
129.33
128.83
128.78
128.77
128.21
128.11
128.04
128.01
127.00
126.95
126.89
125.71
125.03
124.48
124.47
122.85
122.74
119.98
54.21
54.03
53.85
53.67
53.49
29.48
24.13
14.80
0.00
CD2Cl2
grease
160
150
140
130
120
110
100
90
80
70
60
50
40
30
20
10
0
δ(ppm)

4 MASS SPECTRA

TDI-O-4PhBr

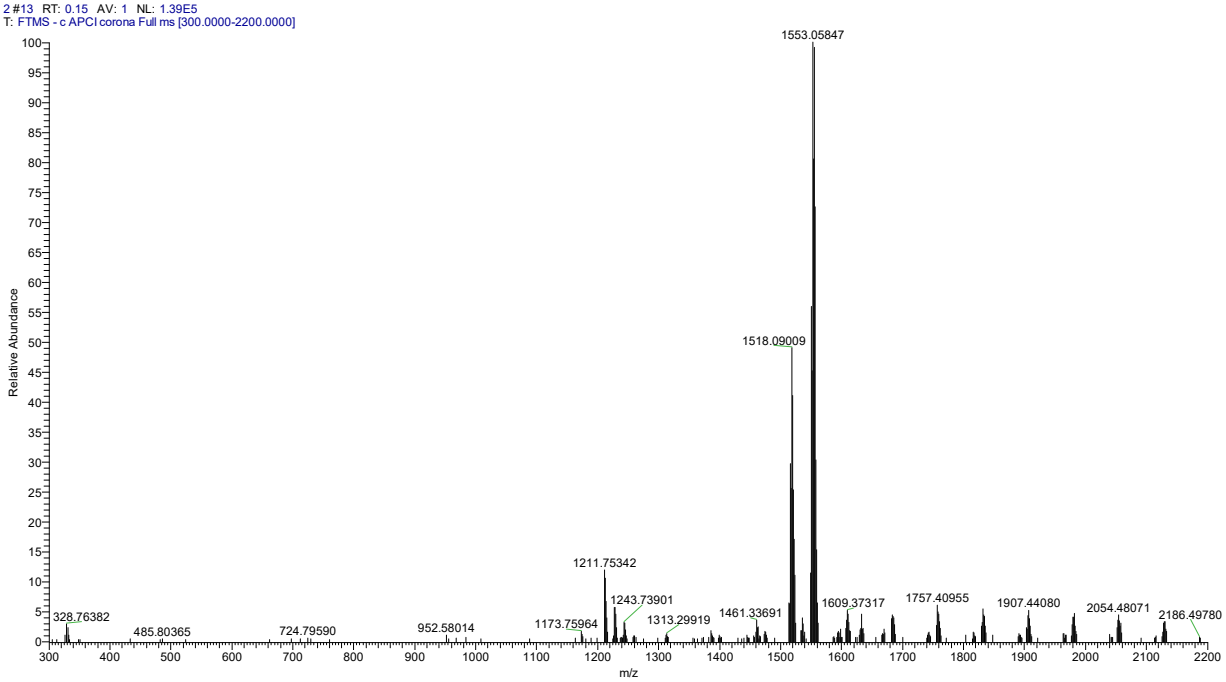

TDI-O-4PhBorate

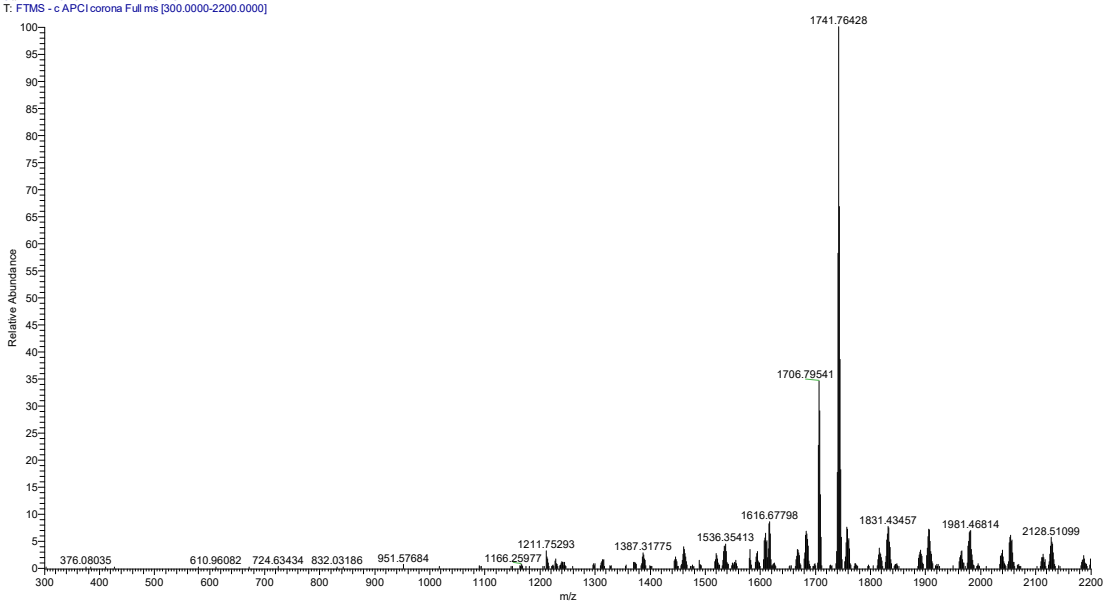

TDI-4(DTE-TPE)

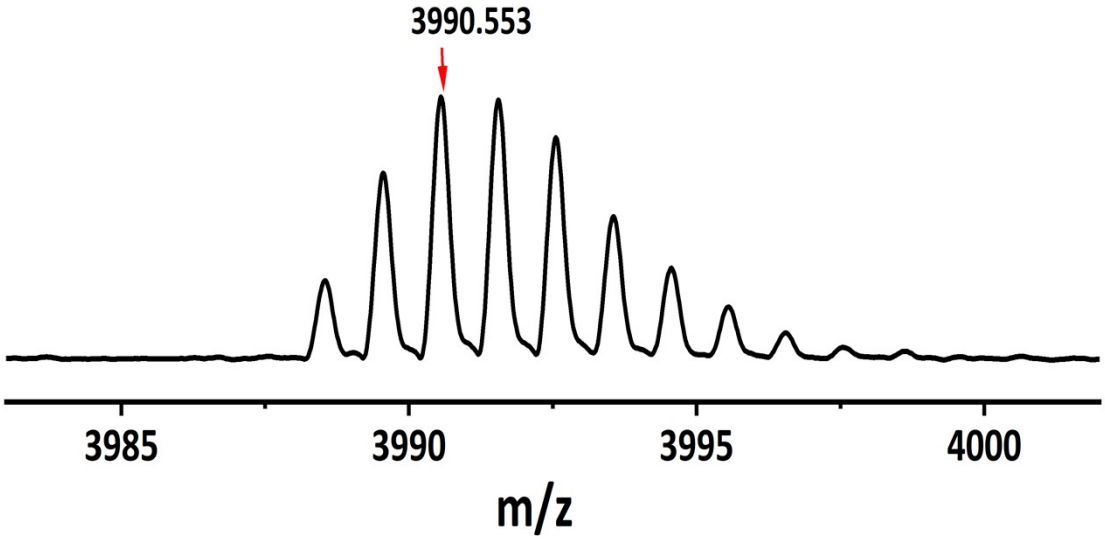

5 REFERENCES

1. C. Li, H. Yan, L.-X. Zhao, G.-F. Zhang, Z. Hu, Z.-L. Huang and M.-Q. Zhu, *Nature Communications*, 2014, **5**, 5709.
2. N.-H. Xie, C. Fan, H. Ye, K. Xiong, C. Li and M.-Q. Zhu, *Acs Applied Materials & Interfaces*, 2019, **11**, 23750-23756.
3. F. Nolde, J. Qu, C. Kohl, N. G. Pschirer, E. Reuther and K. Müllen, *Chemistry – A European Journal*, 2005, **11**, 3959-3967.
4. Q. Bai, B. Gao, Q. Ai, Y. Wu and X. Ba, *Organic Letters*, 2011, **13**, 6484-6487.
5. G. W. T. M. J. Frisch, H. B. Schlegel, G. E. Scuseria, M. A. Robb, J. R. Cheeseman, G. Scalmani, V. Barone, B. Mennucci, G. A. Petersson, H. Nakatsuji, M. Caricato, X. Li, H. P. Hratchian, A. F. Izmaylov, J. Bloino, G. Zheng, J. L. Sonnenberg, M. Hada, M. Ehara, K. Toyota, R. Fukuda, J. Hasegawa, M. Ishida, T. Nakajima, Y. Honda, O. Kitao, H. Nakai, T. Vreven, J. A. Montgomery Jr., J. E. Peralta, F. Ogliaro, M. Bearpark, J. J. Heyd, E. Brothers, K. N. Kudin, V. N. Staroverov, R. Kobayashi, J. Normand, K. Raghavachari, A. Rendell, J. C. Burant, S. S. Iyengar, J. Tomasi, M. Cossi, N. Rega, J. M. Millam, M. Klene, J. E. Knox, J. B. Cross, V. Bakken, C. Adamo, J. Jaramillo, R. Gomperts, R. E. Stratmann, O. Yazyev, A. J. Austin, R. Cammi, C. Pomelli, J. W. Ochterski, R. L. Martin, K. Morokuma, V. G. Zakrzewski, G. A. Voth, P. Salvador, J. J. Dannenberg, S. Dapprich, A. D. Daniels, O. Farkas, J. B. Foresman, J. V. Ortiz, J. Cioslowski and D. J. Fox, Gaussian 09 (Gaussian, Inc., Wallingford, CT), 2009, Revision A.02.
6. A. D. Becke, *The Journal of Chemical Physics*, 1993, **98**, 5648-5652.

7. C. Lee, W. Yang and R. G. Parr, *Physical Review B*, 1988, **37**, 785-789.
8. S. Xu, Q. Yang, Y. Wan, R. Chen, S. Wang, Y. Si, B. Yang, D. Liu, C. Zheng and W. Huang, *Journal of Materials Chemistry C*, 2019, **7**, 9523-9530.
9. C. Li, W.-L. Gong, Z. Hu, M. P. Aldred, G.-F. Zhang, T. Chen, Z.-L. Huang and M.-Q. Zhu, *RSC Advances*, 2013, **3**, 8967-8972.
10. J. Vollbrecht, C. Wiebeler, A. Neuba, H. Bock, S. Schumacher and H. Kitzerow, *The Journal of Physical Chemistry C*, 2016, **120**, 7839-7848.